Biochimica et Biophysica Acta 1848 (2015) 1–7

Contents lists available at ScienceDirect

Biochimica et Biophysica Acta

journal homepage: www.elsevier.com/locate/bbamem

Mechanism for transforming cytosolic SOD1 into integral membrane proteins of organelles by ALS-causing mutations☆

Liangzhong Lim, Xiaowen Lee, Jianxing Song *

Department of Biological Sciences, Faculty of Science, National University of Singapore, Republic of Singapore

ARTICLE INFO

Article history:
Received 24 July 2014
Received in revised form 7 September 2014
Accepted 2 October 2014
Available online 12 October 2014

Keywords:
Amyotrophic lateral sclerosis (ALS)
Superoxide dismutase 1 (SOD1)
Membrane protein
Amphiphilicity
NMR spectroscopy

ABSTRACT

Mutations in superoxide dismutase 1 (SOD1) cause familial amyotrophic lateral sclerosis (FALS), while wild-type SOD1 has been implicated in sporadic ALS (SALS). SOD1 mutants are now recognized to acquire one or more toxicities that include their association with mitochondrial and endoplasmic reticulum membranes but the underlying structural mechanism remains unknown. Here we determine NMR conformations of both wild-type and a truncation mutant (L126Z) of SOD1 in aqueous solution and a membrane environment. The truncation mutant (which causes FALS at very low levels, indicating its elevated toxicity) is highly unstructured in solution, failing to adopt the β-barrel SOD1 native structure. Wild-type SOD1 is also highly unstructured upon reduction of disulfides and depletion of zinc. Most remarkably, both mutant and wild type adopt similar, highly-helical conformations in a membrane environment. Thus, either truncation or depletion of zinc is sufficient to eliminate the native β-barrel structure, and transform cytosolic SOD1 into membrane proteins energetically driven by forming amphiphilic helices in membranes. That zinc-deficiency is sufficient to produce a similar transformation in wild-type SOD1 implies that the wild-type and FALS-linked SOD1 mutants may trigger ALS by a common mechanism.

1. Introduction

Amyotrophic lateral sclerosis (ALS) is the most common motor neuron disease, clinically characteristic of the degeneration of motor neurons in the brain and spinal cord, which leads to paralysis and death within a few years of disease onset. ALS was first described in 1869, which affects approximately 1–2 per 100,000 people worldwide [1–3]. While a list of genes has been linked to the inheritable, or familial ALS (FALS), the cause of sporadic ALS (SALS) accounting for ~90% of ALS cases still remains poorly understood. As sporadic and familial ALS affect the same neurons with the clinical similarities, it is believed that both forms of the disease converge on common pathways or/and involve common factors.

In 1993, superoxide dismutase 1 (SOD1) was identified to be the first gene associated with FALS [4]. Mutations in the SOD1 gene cause the most prevalent form of FALS, accounting for ~20% of total FALS cases. Currently, 177 mutations have been identified within SOD1 that are linked to ALS (http://alsod.iop.kcl.ac.uk/) [5]. Surprisingly, evidence has emerged that a misfolded form of the wild-type SOD1 may be linked to sporadic ALS [3].

SOD1 is a homodimeric enzyme with each subunit adopting a β-barrel composed of eight antiparallel β-strands arranged in a Greek key motif (Fig. 1A), which is highly abundant, comprising ~1% of total protein in neurons. It acts to catalyze the dismutation of superoxide radicals to molecular oxygen and hydrogen peroxide [6]. It is now believed that mutations in SOD1 lead to ALS by a dominant gain of function. Like other neurodegenerative diseases, ALS caused by SOD1 mutants is also characterized by the formation of cytoplasmic aggregates of the mutants, some of which are even resistant to the solubilization by detergents or reducing agents in cell culture models and patients of ALS.

Nevertheless, recently emerging evidence suggests that the toxic SOD1 species are in fact soluble forms of the mutants [3,7,8]. The formation of aggregated SOD1 forms unable to diffuse within the cell may in fact represent a protective mechanism like what is found in other neurodegenerative diseases [3,9,10]. Most strikingly, it has been shown that SOD1 mutants may manifest their cytotoxicity by transforming into proteins associated with the cytoplasmic face of intracellular organelles, including mitochondria [11–13] and endoplasmic reticulum (ER) [14]. However, so far no structural mechanism has been established to rationalize the toxicity gained by the soluble forms of SOD1 mutants as well as their tight association with membranes.

L126Z is a truncation mutant of SOD1 produced by the formation of a stop codon in codon 126 [15], thus resulting in the deletion of the last 28 residues as well as the only disulfide bridge Cys57–Cys146 (Fig. 1B). This truncation leads to a FALS phenotype similar to that observed in patients with missense mutations. Moreover, the truncated enzyme is

☆ The NMR structure and data of the L126Z-SOD1 in DPC have been deposited with PDB code of 2MP3 and BRMB ID of 19962 respectively.

* Corresponding author. Tel.: +65 65161013.
E-mail address: dbssjx@nus.edu.sg (J. Song).

http://dx.doi.org/10.1016/j.bbamem.2014.10.002
0005-2736/

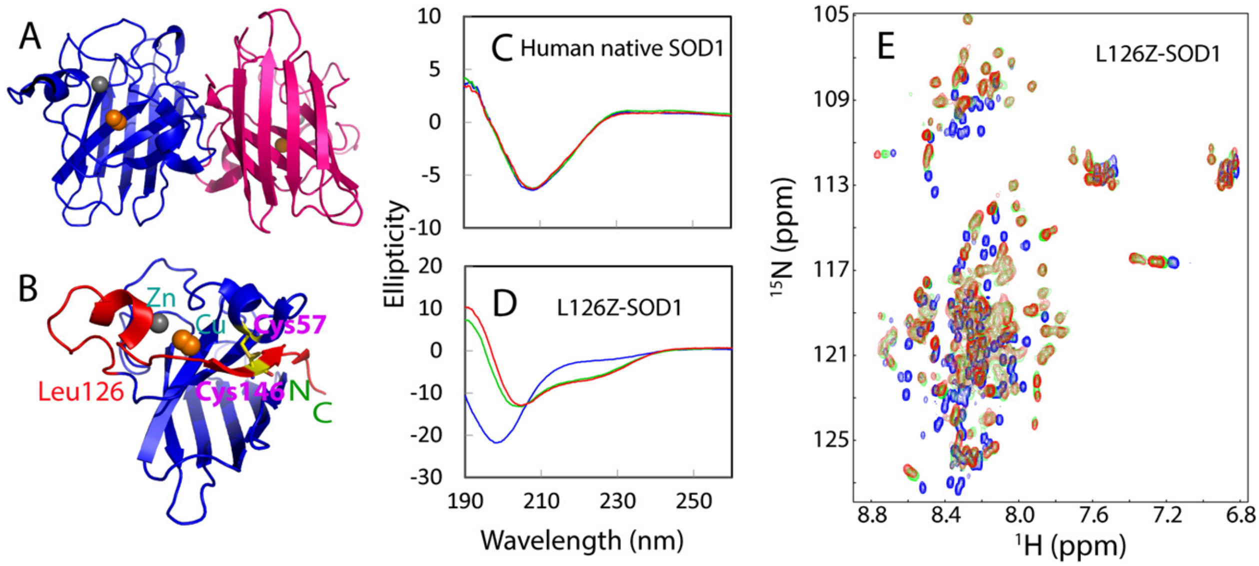

Fig. 1. Structures of human native and L126Z-SOD1. (A) Crystal structure of the dimeric human native SOD1 (PDB code of 2C9U). (B) Structure of the 2C9U monomer with the disulfide bridge Cys57–Cys146, zinc and copper ions labeled. The truncated region in L126Z-SOD1 starting from Leu126 was colored in red. (C) Far-UV CD spectra of the human native SOD1 purified from human erythrocytes (Sigma-Aldrich) in the absence (blue) and in the presence of dodecylphosphocholine (DPC) at molar ratios of 1:100 (green) and 1:200 (red) (SOD1:DPC). (D) Far-UV CD spectra of L126Z-SOD1 in the absence (blue) and in the presence of DPC at molar ratios of 1:100 (green) and 1:200 (red) (L126Z:DPC). (E) Two-dimensional ^{1}H–^{15}N NMR HSQC spectra of L126Z-SOD1 in the absence (blue) and in the presence of DPC at molar ratios of 1:100 (green) and 1:200 (red) (L126Z:DPC).

present at very low levels in FALS patients, indicating its elevated toxicity compared to other mutated SOD1 with only site substitutions [15]. Here by use of circular dichroism (CD) and NMR spectroscopy, we determined conformations and dynamics of the L126Z and wild-type SOD1 sequences in both aqueous solutions and membrane environment, as facilitated by our discovery that previously-thought insoluble proteins could in fact be solubilized in water with minimized salt ions [16–19]. Remarkably, both L126Z-SOD1 and wild-type SOD1 with disulfide reduced and zinc/copper depleted completely lose the β-barrel native structure, becoming highly unstructured in aqueous solutions. Nevertheless, they acquire the capacity to transform into highly-helical states in a membrane environment, as we determined by NMR. Thus, either truncation or zinc depletion is sufficient to eliminate the well-folded SOD1 native structure and to unlock the regions with the intrinsic capacity to interact with membranes as driven by hydrogen bond energetics. Our study not only provides the mechanism for the previous observation that SOD1 mutants were able to transform into proteins with properties of integral membrane proteins of intracellular organelles, but also reveals that the zinc-deficiency is sufficient to produce a similar conformational transformation in wild-type SOD1, thereby implying that the wild-type SOD1 and FALS-linked SOD1 mutants could trigger ALS by a common mechanism.

2. Results

2.1. L126Z becomes highly unstructured and loses the capacity to fold into the native structure

We first collected a far-UV CD spectrum of the native SOD1 purified from human erythrocytes, which is typical of a β-dominant protein (Fig. 1C), consistent with its native β-barrel structure (Fig. 1A). On the other hand, the recombinant L126Z protein was only found in inclusion body, consistent with the in vivo observation that L126Z formed tight aggregates in cells [15]. Nevertheless, once it was purified and lyophilized, it could be solubilized in Milli-Q water at high concentrations (up to 1.2 mM) and remain stable for several weeks without any detectable aggregation. As evidenced by its far-UV CD spectrum with only one maximal negative signal at ~198 nm (Fig. 1D), L126Z is highly unstructured in aqueous solutions. This conclusion is further supported by its ^{1}H-^{15}N HSQC spectrum with very narrow dispersions at both ^{1}H (~0.8 ppm) and ^{15}N (~18 ppm) dimensions (Fig. 1E), which also indicate the absence of the tight tertiary packing [20]. Furthermore, at a low concentration (25 μM), shortly after addition of NaCl (Fig. S1A) or phosphate buffer at neutral pH 7.5 (Fig. S1B), L126Z showed no significant aggregation and remained similarly unstructured. However, the L126Z samples with NaCl and phosphate buffer started to precipitate after ~1 h. This phenomenon has been extensively observed on a variety of other insoluble proteins by us and other groups, suggesting that "insoluble" proteins are in fact soluble to some degree before the formation of tight aggregates in vivo [15–19].

To gain an insight into the residue-specific conformation of L126Z, we achieved its NMR assignments and Fig. 2A presents the (ΔCα–ΔCβ) chemical shift, which is an indicator of the residual secondary structures in unstructured proteins [20]. The small (ΔCα–ΔCβ) chemical shifts for most residues clearly reveal that L126Z-SOD1 is highly disordered in solution, which retains no native β-sheet structure. Furthermore, its heteronuclear NOEs (Fig. 2B), a sensitive indicator of the backbone motions on the ns–ps time scale [18,20], have an average value of −0.03, suggesting that L126Z undergoes highly unrestricted backbone motions. We also collected ^{15}N backbone CPMG relaxation dispersion data and found no significant dispersion (Fig. 2C), indicating the absence of conformational exchanges on the μs–ms time scale with significant chemical shift changes [18]. The presence of weakly-populated helical/loop conformations can be evidenced by the small but positive (ΔCα–ΔCβ) chemical shifts over several segments (Fig. 2A), and further supported by the manifestation of some characteristic NOE connectivities including $d_{NN(i, i+1)}$; $d_{\alpha N(i, i+2)}$ and $d_{\alpha N(i, i+3)}$ (Fig. 2D).

Intriguingly, although the L126Z truncation does not remove the zinc-binding region [6], L126Z loses the capability to fold into the native secondary structures, as evidenced by its far-UV CD spectrum in the presence of Zn^{2+}, which only has the maximal negative signal slightly shifted from 198 to 201 nm (Fig. S2A). Together with its HSQC spectrum which still retains the narrow dispersions but has some HSQC peaks shifted or disappeared (Fig. S2B), it can be concluded that upon introduction of Zn^{2+} L126Z did undergo some conformational changes, or/and μs–ms conformational exchanges, or/and dynamic aggregation [16–19], but was unable to reach the native SOD1 fold with the tight tertiary packing.

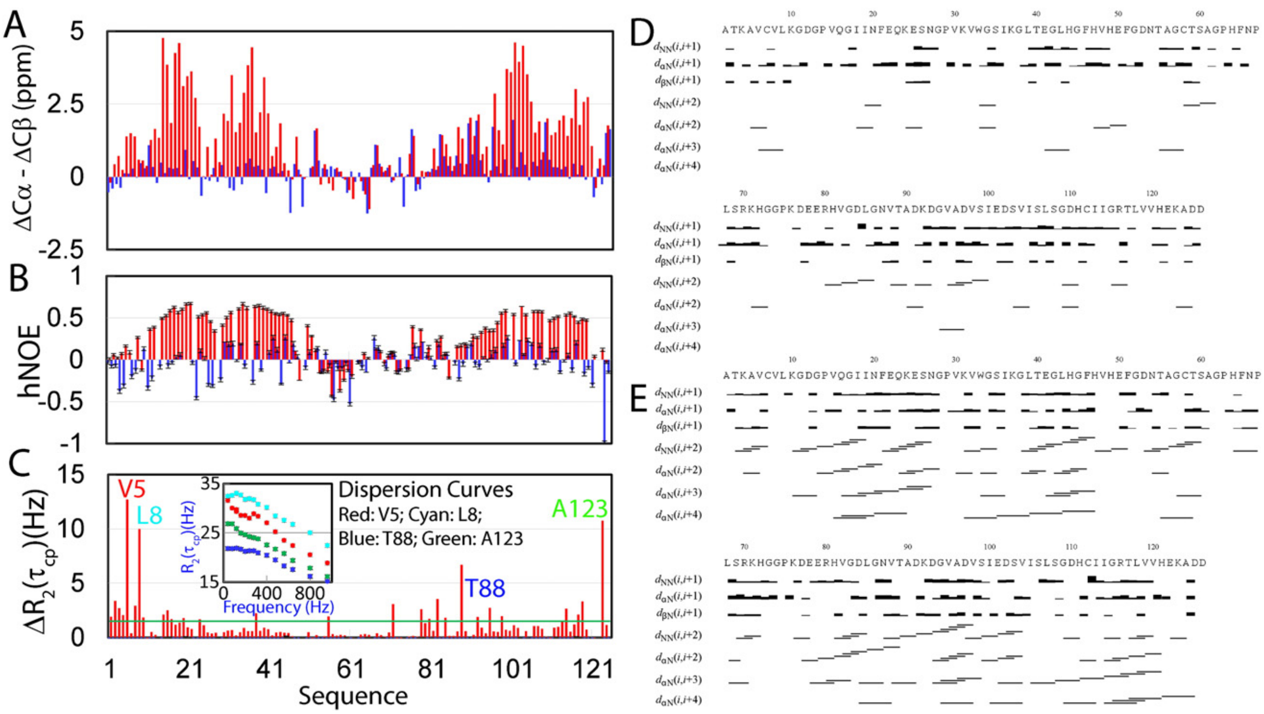

Fig. 2. NMR conformations and dynamics of L126Z in aqueous solution and membrane environment. (A) Residue specific (ΔCα–ΔCβ) chemical shifts of L126Z in aqueous solution (blue) and membrane environment (red). (B) $\{^1H\}$–^{15}N heteronuclear steady-state NOE (hNOE) of L126Z in aqueous solution (blue) and membrane environment (red). (C) Difference of effective transverse relaxation rate $R_2(\tau_{cp})$ at 80 and 960 Hz for L126Z in the membrane environment. Inset: dispersion curves for four residues Val5 (red), Leu8 (cyan), Thr88 (blue) and Ala123 (green). (D) NOE connectivities defining secondary structures of L126Z in aqueous solution, and (E) in the membrane environment.

We have also expressed and purified the full-length human SOD1 by Ni^{2+}-affinity column followed by reverse phase (RP) HPLC under denaturing condition in the presence of 100 mM DTT, with all possible disulfide bridges reduced and zinc/copper depleted, which was designated as FL-SOD1. Surprisingly, FL-SOD1 is also highly unstructured under the same solution conditions for L126Z, as shown by its CD spectrum (Fig. S3A). Superimposition of HSQC spectra shows that FL-SOD1 has only 27 extra HSQC peaks while the rest of peaks are mostly superimposable to those of L126Z-SOD1 (Fig. S3B). This strongly suggests that FL- and L126Z-SOD1 have highly similar conformations over the identical regions. Nevertheless, upon introducing zinc FL-SOD1 transformed into a well-folded state with a far-UV CD spectrum highly similar to that of the native SOD1 purified from human erythrocytes (Fig. S3A). Furthermore, the dispersions of the HSQC spectrum of FL-SOD1 suddenly increased at both ^1H- and ^{15}N-dimensions (Fig. S3C), indicating that FL-SOD1 acquired the tight tertiary packing in the presence of zinc. This is in a complete agreement with the previous report that the presence of zinc ion alone was sufficient to maintain the native SOD1 structure even without copper and disulfide bridge [21]. It has been widely accepted that to fold into the native structure, SOD1 has first to acquire zinc ions from an unknown source, followed by subsequent copper transfer from the SOD1-specific copper chaperone and coupled formation of the disulfide bridge [21,22]. We thus assessed the conformational change upon adding copper into FL-SOD1 without the pre-existence of zinc by HSQC. It appeared that copper could indeed bind some residues as indicated by the shift of a small portion of HSQC peaks (Fig. S3D). However, the copper binding failed to trigger the folding of FL-SOD1 into the native structure as the HSQC spectral dispersions remained largely unchanged. Furthermore, visible aggregates formed half an hour after addition of copper. This suggests that the zinc-deficiency is sufficient to block the correct folding of SOD1 of the wild-type sequence as well as to prevent the subsequent copper-loading and disulfide formation [21,22].

The loss of the capacity to fold into the native SOD1 structure thus explains why L126Z is highly insoluble in cells. Even in the presence of zinc, L126Z still remains highly unstructured without the tight tertiary packing. As such, many hydrophobic patches of L126Z are improperly exposed to the bulk solvent, which will lead to the unavoidable aggregation in vivo with high ion concentrations (~150 mM), by the same mechanism which have been previously proposed for other insoluble proteins [16,17]. Similarly, as under zinc-deficiency the FL-SOD1 is also highly unstructured like L126Z-SOD1, it is therefore expected to undergo severe aggregation in vivo as extensively observed [3].

2.2. L126Z-SOD1 gains the capacity to transform into a helical state in a membrane environment

Previously, SOD1 mutants have been characterized to transform into integral membrane proteins to become associated onto the membranes of intracellular organelles such as mitochondria and ER [11–14]. Therefore, here we assessed the potential of L126Z to interact with membranes by use of the lipid mimetic dodecylphosphocholine (DPC), which can form the small micelle suitable for high-resolution NMR studies. As shown in Fig. 1C, the native SOD1 purified from human erythrocytes has almost the same CD spectra in the absence and in the presence of DPC, indicating that DPC is unable to trigger any significant structure change of the native SOD1. By a sharp contrast, upon adding DPC, L126Z undergoes a transition from an unstructured state into a highly helical state (Fig. 1D), with the transition largely completed at a molar ratio of 1:100 (L126Z:DPC). This transition is further confirmed by DPC titrations as monitored by HSQC spectra (Fig. 1E), which show that upon adding DPC, the majority of HSQC peaks shift dramatically, but the shifting for most peaks completed at a molar ratio of 1:100. Furthermore, in the DPC micelle L126Z showed no severe aggregation for at least 1 h at a protein concentration of 150 μM and even in the presence of 10 mM phosphate buffer pH 7.5 (Fig. S1C).

To characterize the residue-specific conformations, we also successfully achieved NMR assignments of L126Z in the DPC micelle. In the membrane environment, many residues of L126Z become highly-helical as evidenced by their large and positive (ΔCα–ΔCβ) chemical shifts, including Val14-Glu21, Lys32-His43, and Ile99-Val119 (Fig. 2A). Moreover, hNOE values for most residues become positive, with an average value of 0.3. In particular, many residues forming helices have hNOE values larger than 0.5 (Fig. 2B), indicating that in the membrane environment the ps–ns backbone motions of residues become largely restricted. On the other hand, as indicated by both chemical shifts and hNOEs, most residues over Glu49-Asp90 appear to still have no stable and regular secondary structures and the ps–ns backbone motions largely unrestricted. Furthermore, in the membrane environment many L126Z residues, in particular Val5, Leu8, Thr88 and Ala123, undergo μs–ms conformational exchanges as reflected by ^{15}N backbone CPMG relaxation dispersion data (Fig. 2C). In particular, the transformation of L126Z into a highly helical state in the membrane environment is unambiguously evident by the manifestation of a large number of NOE connectivities characteristic of the helical conformation including $d_{NN(i,\ i\ +\ 1)}$, $d_{NN(i,\ i\ +\ 2)}$, $d_{\alpha N(i,\ i\ +\ 2)}$, $d_{\alpha N(i,\ i\ +\ 3)}$ and even $d_{\alpha N(i,\ i\ +\ 3)}$ (Fig. 2E).

Very interestingly, upon adding DPC, FL-SOD1 (with all possible disulfide bridge reduced and zinc/copper depleted) also undergoes a transition into a helical state with a far-UV CD spectrum similar to that of L126Z in DPC (Fig. S4A). Strikingly, superimposition of HSQC spectra of the DPC-bound FL- and L126Z-SOD1 shows that except for 28 extra peaks, the rest of HSQC peaks of FL-SOD1 are superimposable to those of L126Z-SOD1 (Fig. S4B). This strongly suggests that even in the DPC micelle, FL- and L126Z-SOD1 have highly similar conformations over the identical regions. Nevertheless, in the presence of zinc, FL-SOD1 folded into the native structure and was no longer able to transform into a helical state even in the presence of DPC up to a molar ratio of 1:200 (Fig. S4C).

2.3. NMR conformation of L126Z-SOD1 in the membrane environment

To visualize the helical conformation of L126Z in the membrane environment, we modeled its NMR structure with 106 dihedral angle and 608 distance constraints derived from 296 sequential and 312 medium-range NOEs (Fig. S5A), followed by the energy minimization. Fig. 3A presents the lowest-energy NMR structure, which is composed of four well-formed helices: two on the N-half of L126Z over residues Pro13-As26 and Leu38-His48, and other on the C-half over Val97-His110 and Ile112-H120, connected by a long and unstructured loop over residues Glu49-Asp96. Interestingly, all four helices are highly amphiphilic, with one side of helices constituted by hydrophobic residues and another side by hydrophilic ones (Fig. 3B–E). As such, the membrane-embedded L126Z-SOD1 molecule has relatively polar surfaces on the one side (Fig. 3F) and hydrophobic on another side (Fig. 3G). This implies that like other amphiphilic proteins, upon partitioning into membrane environments L126Z also has its amphiphilic helices mostly sitting in between the interface of the polar and hydrophobic phases of the membranes. Consequently, the hydrophobic side chains of the amphiphilic helices insert into the hydrophobic hydrocarbon phase of the membrane while the polar side chains are either embedded in the polar headgroup phase, or even exposed to the bulk solvent [23,24]. Indeed, we further explored the accessibility of the L12Z residues in the membrane environment by titrations with two paramagnetic agents: namely manganese and gadodiamide as we previously performed on the DPC-bound P56S-MSP [18]. Upon titrating with gadodiamide, HSQC peaks of most loop residues, terminal and several residues on the helices disappeared or have the intensities significantly reduced (Fig. S4B), implying that these residues are mostly exposed to the bulk solvent (Fig. 3H). On the other hand, at high manganese concentrations (>6 mM), the peak intensities of almost all L126Z residues decreased dramatically, implying that no L126Z residues are deeply buried in the hydrocarbon phase [18]. Also as shown in Fig. 3H, most residues with hNOE larger than 0.5 are located on the well-formed helices. On the other hand, three out of four residues with significant μs–ms conformational exchanges are over the N- and C-termini (Fig. 3I). It is also interesting to note that the polar surface of the N-half is largely positively-charged while that of the C-half is negatively-charged. This unique electrostatic property may play a key role in determining the specificity of interacting with membranes.

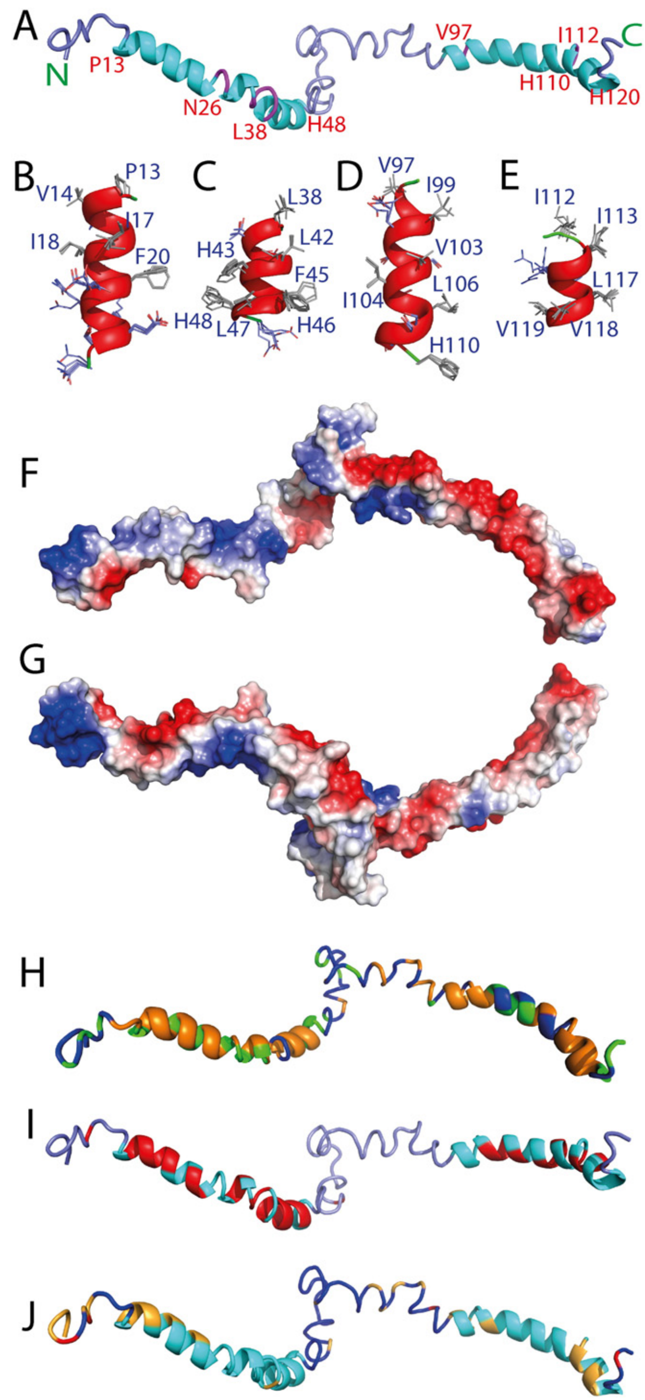

Fig. 3. NMR structure of L126Z in the membrane environment. (A) The lowest-energy NMR structures of L126Z in the membrane environment, with starting and ending residues of four helices labeled. (B)–(E) Superimposition of helices 1–4 of the five lowest-energy L126Z NMR structures, with side chains displayed and particularly hydrophobic and aromatic side-chains labeled. (F) Electrostatic surface of L126Z: positively charged (blue), negatively charged (red) and non-polar (gray). (G) Electrostatic surface with a 180 degree rotation of (F) along x-axis. (H) NMR structure with residues having relative intensity of HSQC peak < 0.3 colored in blue, upon adding 10 mM gadodiamide (Fig. S4B). Green is used to indicate Pro residues, or residues with missing HSQC peaks, or residues without precise peak intensities due to the peak overlap. (I) NMR structure with residues having hNOE > 0.5 colored in red. (J) NMR structure with residues having $\Delta R_2(\tau_{cp})$ > 1.5 colored in bright brown, and >5 in red (Fig. 3C).

So what is the driving force for the insertion of the highly unstructured L126Z-SOD1 into the membrane environment? Previously, it has been established that in the membrane environments, the formation of hydrogen bonds between protein backbone atoms and bulk water molecules will be significantly blocked [23,24]. As a consequence, protein backbones prefer adopting helix which allows the formation of a large number of backbone hydrogen bonds. This will thus result in gain of hydrogen bond energetics which drive the partitioning of the unstructured proteins with high hydrophobicity or/and amphiphilicity from aqueous solutions into membrane environments [23,24].

Due to the lacking of any long-range NOEs, the orientations of the four helices could not be defined in the DPC-embedded NMR structures of L126Z. This has been previously observed on the DPC-embedded structure of the 125-residue ALS-causing P56S-MSP domain [18]. Although we have put extensive efforts to further determine the three-dimensional topology of the P56S-MSP in the DPC micelle by spin-labeling at 7 locations, we found that the topology appeared to be mostly constrained by the micelle shape and therefore might significantly vary in real biological membranes [18]. On the other hand, due to the size limitation for liquid NMR spectroscopy, we are not able to characterize the conformations of L126Z in liposomes or real biological membranes. However, the lack of the tight tertiary packing among different helices appears to be the characteristics of dynamically-interacting membrane proteins by forming amphiphilic helix [18,23,24]. In fact, this lack may offer an advantage/flexibility for these proteins to adjust the orientations of helical segments to adapt onto different membranes [18,25–27]. Indeed, even in the SDS micelle, α-synuclein has been shown to own a high plasticity in adopting differential conformations as revealed by NMR and MD simulations [25–27].

3. Discussion

Here we show that although the L126Z truncation only removes the electrostatic loop, β-strand 8 and disulfide bridge [6,15], L126Z-SOD1 abolishes the native β-barrel fold and becomes predominantly unstructured with highly unrestricted ps–ns backbone motions in aqueous solutions. Consequently, L126Z-SOD1 becomes fundamentally indistinguishable from the membrane-active toxin mellitin from honeybee venom [23,24] and α-synuclein causing Parkinson's disease [9, 25–27], both of which are intrinsically unstructured and prone to aggregation in aqueous buffers, but transform into amphiphilic helices upon encountering membranes.

Surprisingly, FL-SOD1 with all possible disulfide bridges reduced and zinc/copper depleted is also unstructured with the identical region adopting the conformation very similar to that of L126Z-SOD1. Nevertheless, upon adding zinc FL-SOD1 was able to fold into the native structure with tight tertiary packing while L126Z-SOD1 failed. On the other hand, L126Z-SOD1 gains the capacity to partition into membranes by transforming into a highly helical state with the formation of four amphiphilic helices (Fig. 4A). More specifically, the first four β-strands in the native SOD1 fold transform into the N-terminal two helices formed in the membrane environment (Fig. 4B); while part of 5th β-strand, a short helix together with 6th and 7th β-strands become the C-terminal two helices (Fig. 4D). A short helix, zinc-binding region and part of 5th β-strand become a long middle loop without stable and regular secondary structures (Fig. 4C), which is largely exposed to the bulk solvent even in the membrane environment. So how is this chameleon transformation possible? Examination of the L126Z sequence reveals that it contains short segments which have either relatively high hydrophobicity (Fig. S4E), or/and amphiphilicity as universally observed on all proteins [28] (Fig. S4F). In the native SOD1 structure, the hydrophobic residues within the regions transforming into helices in the membrane environment are mostly involved in forming a hydrophobic core which stabilizes the native β-barrel and is largely shielded from the bulk solvent (Fig. S5C). Upon truncation or depletion of zinc, the tight packing of SOD1 is dramatically disrupted and consequently these hydrophobic patches become largely accessible to the bulk solvent. The exposed hydrophobic patches will drive severe aggregation of L126Z in aqueous solutions with high concentrations of ions [16–19]. On the other hand, upon encountering a membrane surface composed of both polar and hydrophobic (the lipid underneath the head groups) phases, these hydrophobic/amphiphilic patches will form amphiphilic helices, thus gaining the capacity to partition into membranes as mostly driven by hydrogen bond energetics [17,18,23,24]. In other words, the driving forces for aggregation and partition into membranes are at least partly overlapped [17,18].

Recently, additional to classically acting as membrane-active toxins such as honeybee mellitin [18,24,25], proteins containing amphiphilic helices have been increasingly identified to play key roles in a variety of essential physiological processes associated with biological membranes, such as controlling membrane curvature, fusion and trafficking [9,18,29,30]. However, different from the classic transmembrane helix which has high hydrophobicity over the whole surface and is thus deeply embedded in the hydrophobic hydrocarbon phase of membranes, the amphiphilic helix mostly sits in between the polar headgroup and hydrophobic hydrocarbon phases of membranes. As such, proteins with high amphiphilicity interact with membranes rather dynamically, characteristic of the absence of tight tertiary packing and the presence of significant motions on both ps–ns and μs–ms time scales [18,23–27,29,30]. However, the high dynamics may not only offer an advantage/plasticity for the disease-causing proteins to rearrange the orientation of the helical fragments to adapt onto different membranes with diverse compositions and curvature etc., but also to enhance their damaging effects to membranes.

Our present study not only provides the underlying mechanism for the observation that SOD1 mutants were able to transform into apparently integral membrane proteins to become associated with intercellular organelle membranes [11–14], but also rationalizes the emerging evidence that the wild-type SOD1 can trigger SALS pathogenesis. As we reveal here, L126Z- and FL-SOD1 with disulfide reduced and zinc/copper depleted share very similar conformations over the identical 125 residues both in aqueous solutions and in a membrane environment. This implies that although FL-SOD1 triggers SALS but L126Z-SOD1 causes FALS, the two may converge on a common mechanism in attacking membranes. However, once zinc is loaded to FL-SOD1, it folds into the native structure which is no longer able to interact with membranes. This highlights the extremely-critical role of zinc in switching the toxic unstructured state into the non-toxic native state for the wild-type SOD1, consistent with the recent results [14]. Furthermore, this also implies that to increase the effective cellular concentration of zinc might represent an important therapy for SALS patients caused by the wild-type SOD1. In this regard, the SOD1 mutants losing the ability to bind zinc may become similarly unstructured and thus have the capacity to interact with membranes as L126Z- and FL-SOD1. For other SOD1 mutants, which have previously been shown to also own impaired post-translational folding [22], the delayed formation of the native structure is likely to increase the probability for their unstructured intermediates to shift toward interacting with membranes. Now we are focused on testing this hypothesis.

Previously, partly-soluble proteins causing human diseases have been demonstrated to insert into membranes by forming amphiphilic helices, which include prions of spongiform transmissible encephalopathies [31], amyloid beta-peptides of Alzheimer's disease [32], tau tangles of Alzheimer's disease [33], α-synuclein of Parkinson's disease [9, 25–27], huntingtin of Huntington's disease [34], and the islet amyloid polypeptide of type II diabetes [35]. Now with our earlier discoveries [16–19] in which we were able to show that previously-thought "completely insoluble proteins" resulted from the mutations/truncations of well-folded proteins are in fact soluble to some degree before forming the tight aggregates. In particular, the soluble forms of these "completely insoluble proteins" gain strong potential to interact with membranes [17–19]. As a consequence, with our results added in, a

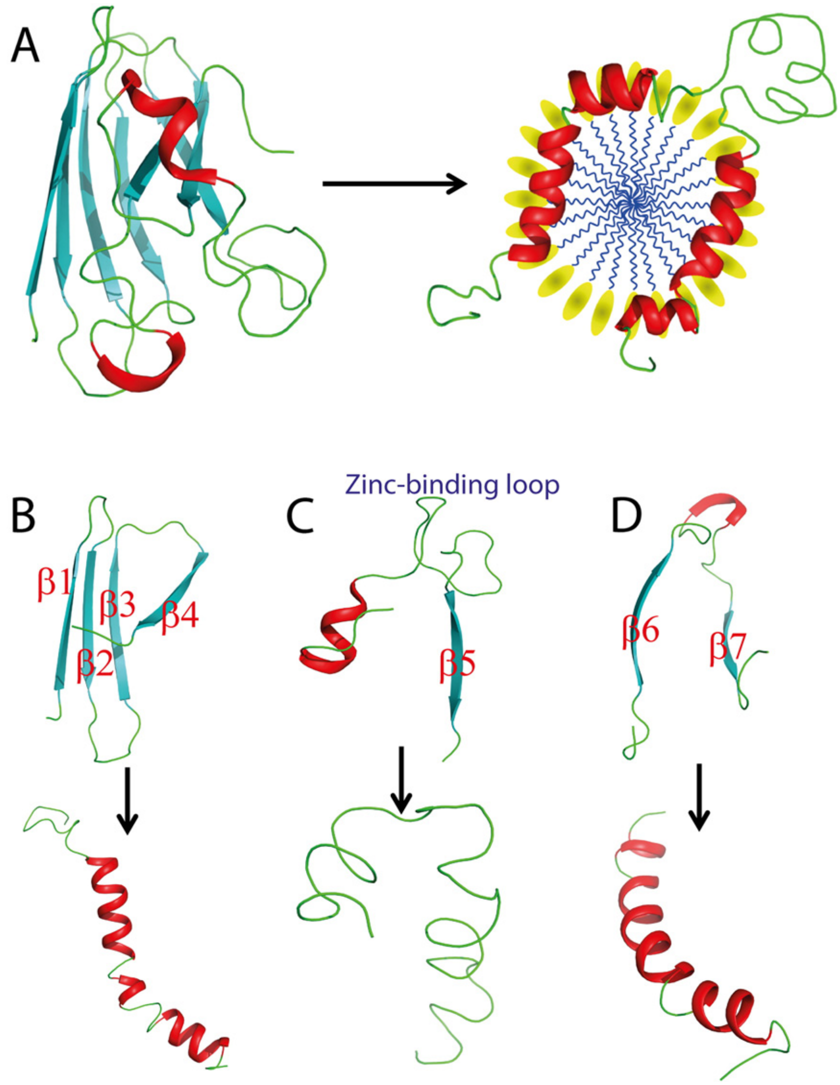

Fig. 4. Chameleon transformation of L126Z-SOD1 from the cytosolic β-barrel fold into the membrane-embedded helical state. (A) The L126Z truncation leads to the chameleon transformation from the native SOD1 β-barrel structure in the cytosol into a highly-helical state in the DPC micelle. The yellow ellipsoids are used for representing the polar headgroups of DPC while the blue lines for its hydrophobic hydrocarbon chains. The amphiphilic helices of L126Z are sitting in between the polar and hydrophobic phases of the DPC micelle. (B) The first four β-strands in the native SOD1 structure transform into the N-terminal two helices in the membrane environment. (C) A short helix, zinc-binding region and part of 5th β-strand become a long loop without any stable and regular secondary structures. (D) Part of 5th β-strand, 6th and 7th β-strands, together with a short helix, become the C-terminal two helices in the membrane environment.

general conclusion can now be reached that the aggregated proteins linked to human neurodegenerative diseases all share the common potential to interact with membranes regardless of being “partly” or “completely” insoluble.

An interaction with membranes thus represents a common mechanism known so far for these proteins, which have no consensus in physiological functions but can trigger a diverse spectrum of human diseases. In fact, previously the underlying mechanisms for initiating pathogenesis by interacting with membranes have been extensively investigated, which are involved in almost all membrane-associated processes: 1) disruption of membrane structures and dynamics such as by forming ion channels/pores or aggregates within membranes [17,18,23,24,34,36]; or/and 2) perturbation of membrane-anchored signal pathways [14] or machineries such as ion channels [13]; or/and 3) interference in the membrane remodeling such as shaping, trafficking and fusion [9,18,37]. These mechanisms are not necessarily mutually exclusive and may act simultaneously in many cases. Indeed, remodeling of membrane shapes by a very weak binding (with Kd ~ mM) has been proposed for α-synuclein [37], implying that membrane-associated physiological processes can be perturbed by proteins with potential to interact with membranes and many such interactions might still remain unrecognized in cells.

4. Methods

The native SOD1 purified from human erythrocytes was purchased from Sigma-Aldrich. FL- and L126Z-SOD1 were expressed in *Escherichia coli* BL21 (DE3) cells (Novagen) and subsequently purified by Ni^{2+}-affinity and HPLC chromatography. The purity of the recombinant proteins was checked by SDS-PAGE gels and verified by a Voyager STR matrix-assisted laser desorption ionization time-of-flight-mass spectrometer (Applied Biosystems), as well as NMR assignments.

All circular dichroism (CD) experiments were performed on a Jasco J-810 spectropolarimeter and NMR experiments were acquired on an 800 MHz Bruker Avance spectrometer equipped with pulse field gradient units. Detailed descriptions of CD and NMR experiments, as well as structure modeling are provided in SI Methods.

Author contributions

X.S. and L.Z.L., designed research; L.Z.L., J.X.S. and X.W.L., performed research; L.Z.L. and J.X.S., analyzed data; J.X.S. wrote the paper.

Acknowledgement

We thank Mr. Hongmeng Yew and Ms. Linlin Miao for preparing the samples, as well as Dr. Jingsong Fang for assistance in acquiring NMR spectra. The study is supported by the Ministry of Education of Singapore (MOE) Tier 2 Grant MOE 2011-T2-1-096 (R154-000-525-112) to Jianxing Song. The funders had no role in study design, data collection and analysis, decision to publish, or preparation of the manuscript.

Appendix A. Supplementary data

Supplementary data to this article can be found online at http://dx.doi.org/10.1016/j.bbamem.2014.10.002.

References

[1] L.I. Bruijn, T.M. Miller, D.W. Cleveland, Unraveling the mechanisms involved in motor neuron degeneration in ALS, Annu. Rev. Neurosci. 27 (2004) 723–749.
[2] S. Da Cruz, D.W. Cleveland, Understanding the role of TDP-43 and FUS/TLS in ALS and beyond, Curr. Opin. Neurobiol. 21 (6) (2011) 904–919.
[3] M.S. Rotunno, D.A. Bosco, An emerging role for misfolded wild-type SOD1 in sporadic ALS pathogenesis, Front. Cell. Neurosci. 7 (2013) 253.
[4] D.R. Rosen, T. Siddique, D. Patterson, D.A. Figlewicz, P. Sapp, et al., Mutations in Cu/Zn superoxide dismutase gene are associated with familial amyotrophic lateral sclerosis, Nature 362 (6415) (1993) 59–62.
[5] O. Abel, J.F. Powell, P.M. Andersen, A. Al-Chalabi, ALSoD: a user-friendly online bioinformatics tool for amyotrophic lateral sclerosis genetics, Hum. Mutat. 33 (9) (2012) 1345–1351.
[6] J.J. Perry, D.S. Shin, E.D. Getzoff, J.A. Tainer, The structural biochemistry of the superoxide dismutases, Biochim. Biophys. Acta 1804 (2) (2010) 245–262.
[7] P. Zetterström, H.G. Stewart, D. Bergemalm, P.A. Jonsson, K.S. Graffmo, et al., Soluble misfolded subfractions of mutant superoxide dismutase-1s are enriched in spinal cords throughout life in murine ALS models, Proc. Natl. Acad. Sci. U. S. A. 104 (35) (2007) 14157–14162.
[8] T.E. Brotherton, Y. Li, J.D. Glass, Cellular toxicity of mutant SOD1 protein is linked to an easily soluble, non-aggregated form in vitro, Neurobiol. Dis. 49C (2012) 49–56.
[9] P.K. Auluck, G. Caraveo, S. Lindquist, α-Synuclein: membrane interactions and toxicity in Parkinson's disease, Annu. Rev. Cell Dev. Biol. 26 (2010) 211–233.
[10] R.A. Bodner, T.F. Outeiro, S. Altmann, M.M. Maxwell, S.H. Cho, et al., Pharmacological promotion of inclusion formation: a therapeutic approach for Huntington's and Parkinson's diseases, Proc. Natl. Acad. Sci. U. S. A. 103 (11) (2006) 4246–4251.
[11] C. Vande Velde, T.M. Miller, N.R. Cashman, D.W. Cleveland, Selective association of misfolded ALS-linked mutant SOD1 with the cytoplasmic face of mitochondria, Proc. Natl. Acad. Sci. U. S. A. 105 (10) (2008) 4022–4027.
[12] J. Liu, C. Lillo, P.A. Jonsson, C. Vande Velde, C.M. Ward, et al., Toxicity of familial ALS-linked SOD1 mutants from selective recruitment to spinal mitochondria, Neuron 43 (1) (2004) 5–17.
[13] A. Israelson, N. Arbel, S. Da Cruz, H. Ilieva, K. Yamanaka, et al., Misfolded mutant SOD1 directly inhibits VDAC1 conductance in a mouse model of inherited ALS, Neuron 67 (4) (2010) 575–587.
[14] K. Homma, T. Fujisawa, N. Tsuburaya, N. Yamaguchi, H. Kadowaki, et al., SOD1 as a molecular switch for initiating the homeostatic ER stress response under zinc deficiency, Mol. Cell 52 (1) (2013) 75–86.
[15] J.S. Zu, H.X. Deng, T.P. Lo, H. Mitsumoto, M.S. Ahmed, et al., Exon 5 encoded domain is not required for the toxic function of mutant SOD1 but essential for the dismutase activity: identification and characterization of two new SOD1 mutations associated with familial amyotrophic lateral sclerosis, Neurogenetics 1 (1) (1997) 65–71.
[16] J. Song, Insight into “insoluble proteins” with pure water, FEBS Lett. 583 (6) (2009) 953–959.
[17] J. Song, Why do proteins aggregate? “Intrinsically insoluble proteins” and “dark mediators” revealed by studies on “insoluble proteins” solubilized in pure water, F1000Res. 2 (2013) 94.
[18] H. Qin, L. Lim, Y. Wei, G. Gupta, J. Song, Resolving the paradox for protein aggregation diseases: a common mechanism for aggregated proteins to initially attack membranes without needing aggregates, F1000Res. 2 (2013) 221.
[19] H. Qin, W. Wang, J. Song, ALS-causing P56S mutation and splicing variation on the hVAPB MSP domain transform its β-sandwich fold into lipid-interacting helical conformations, Biochem. Biophys. Res. Commun. 431 (3) (2013) 398–403.
[20] H.J. Dyson, P.E. Wright, Unfolded proteins and protein folding studied by NMR, Chem. Rev. 104 (8) (2004) 3607–3622.
[21] L. Banci, I. Bertini, F. Cantini, N. D'Amelio, E. Gaggelli, Human SOD1 before harboring the catalytic metal: solution structure of copper-depleted, disulfide-reduced form, J. Biol. Chem. 281 (4) (2006) 2333–2337.
[22] C.K. Bruns, R.R. Kopito, Impaired post-translational folding of familial ALS-linked Cu, Zn superoxide dismutase mutants, EMBO J. 26 (3) (2007) 855–866.
[23] S.H. White, W.C. Wimley, Membrane protein folding and stability: physical principles, Annu. Rev. Biophys. Biomol. Struct. 28 (1999) 319–365.
[24] A.S. Ladokhin, S.H. White, Folding of amphipathic alpha-helices on membranes: energetics of helix formation by melittin, J. Mol. Biol. 285 (4) (1999) 1363–1369.
[25] R. Bussell Jr., T.F. Ramlall, D. Eliezer, Helix periodicity, topology, and dynamics of membrane-associated alpha-synuclein, Protein Sci. 14 (4) (2005) 862–872.
[26] T.S. Ulmer, A. Bax, N.B. Cole, R.L. Nussbaum, Structure and dynamics of micelle-bound human alpha-synuclein, J. Biol. Chem. 280 (10) (2005) 9595–9603.
[27] P. Mazumder, J.E. Suk, T.S. Ulmer, Insight into α-synuclein plasticity and misfolding from differential micelle binding, J. Phys. Chem. B 117 (39) (2013) 11448–11459.
[28] S.Y. Lee, W. Parker, Amphiphilic α-helical potential: a putative folding motif adding few constraints to protein evolution, J. Mol. Evol. 73 (3–4) (2011) 166–180.
[29] R. Jahn, T.C. Südhof, Membrane fusion and exocytosis, Annu. Rev. Biochem. 68 (1999) 863–911.
[30] M.C. Lee, L. Orci, S. Hamamoto, E. Futai, M. Ravazzola, R. Schekman, Sar1p N-terminal helix initiates membrane curvature and completes the fission of a COPII vesicle, Cell 122 (4) (2005) 605–617.
[31] K. Elfrink, J. Ollesch, J. Stöhr, D. Willbold, D. Riesner, et al., Structural changes of membrane-anchored native PrP(C), Proc. Natl. Acad. Sci. U. S. A. 105 (31) (2008) 10815–10819.
[32] H. Shao, S. Jao, K. Ma, M.G. Zagorski, Solution structures of micelle-bound amyloid beta-(1–40) and beta-(1–42) peptides of Alzheimer's disease, J. Mol. Biol. 285 (2) (1999) 755–773.
[33] G. Künze, P. Barré, H.A. Scheidt, D. Eliezer, et al., Binding of the three-repeat domain of tau to phospholipid membranes induces an aggregated-like state of the protein, Biochim. Biophys. Acta 1818 (9) (2012) 2302–2313.
[34] K.B. Kegel, E. Sapp, J. Yoder, B. Cuiffo, L. Sobin, et al., Huntingtin associates with acidic phospholipids at the plasma membrane, J. Biol. Chem. 280 (43) (2005) 36464–36473.
[35] J.R. Brender, S. Salamekh, A. Ramamoorthy, Membrane disruption and early events in the aggregation of the diabetes related peptide IAPP from a molecular perspective, Acc. Chem. Res. 45 (3) (2012) 454–462.
[36] B.L. Kagan, H. Jang, R. Capone, F. Teran Arce, S. Ramachandran, et al., Antimicrobial properties of amyloid peptides, Mol. Pharm. 9 (4) (2012) 708–717.
[37] Z. Jiang, M. de Messieres, J.C. Lee, Membrane remodeling by α-synuclein and effects on amyloid formation, J. Am. Chem. Soc. 135 (43) (2013) 15970–15973.